Metabolomics (2015) 11:1733–1742
DOI 10.1007/s11306-015-0826-3

ORIGINAL ARTICLE

Matrix effect on chemical isotope labeling and its implication in metabolomic sample preparation for quantitative metabolomics

Wei Han[1] · **Liang Li**[1]

Received: 23 April 2015 / Accepted: 19 June 2015 / Published online: 14 July 2015

Abstract Matrix effect from various constituents in biological samples can reduce the accuracy of quantitative metabolomics. Differential chemical isotope labeling liquid chromatography mass spectrometry (MS) can overcome the matrix effect on MS detection based on measuring the intensity ratios of metabolite peak pairs detected in a mixture of a light-isotope labeled sample and a heavy-isotope labeled reference sample. However, the chemical labeling process itself may encounter matrix effect which can influence the overall quantitative results. In this work, we report the effects of salts and buffers commonly present in metabolomic samples on dansylation labeling. It is shown that high concentrations of NaCl and phosphate buffer (>50 mM) or PBS can reduce or enhance the labeling efficiencies of metabolites. By maintaining similar matrix contents in an individual sample versus a reference sample, relative quantification of metabolites can be performed without compromising the metabolomic profiling results. For samples containing varying amounts of high salts such as urine, we demonstrate that the matrix effect can be largely overcome by diluting the original sample before dansylation labeling (e.g., fourfold dilution for urine).

Keywords Matrix effect · Sample preparation · Chemical isotope labeling · LC–MS · Quantitative metabolomics

Electronic supplementary material The online version of this article (doi:10.1007/s11306-015-0826-3) contains supplementary material, which is available to authorized users.

✉ Liang Li
liang.li@ualberta.ca

[1] Departments of Chemistry, University of Alberta, Edmonton, AB, Canada

1 Introduction

Chemical isotope labeling liquid chromatography mass spectrometry (CIL LC–MS) is an enabling analytical platform for generating comprehensive and quantitative metabolomic profiles for metabolomics research (Guo and Li 2009). Using a proper labeling reagent to react with a class of metabolites (e.g., all amine-containing metabolites), a chemical-group-based submetabolome can be analyzed with improved LC separation and enhanced MS sensitivity to generate a comprehensive profile of the submetabolome (Guo and Li 2009, 2010). By combining the results of different submetabolomes generated using labeling reagents targeting different chemical groups, a large coverage of the entire metabolome may be achieved (Fu et al. 2013). A growing number of CIL reagents have been developed for targeted metabolite analysis or group-based submetabolome profiling (Tang and Guengerich 2010; Yuan et al. 2011; Toyo'oka 2012; Dai et al. 2012; Tayyari et al. 2013; Leng et al. 2013; Bueschl et al. 2013; Bruheim et al. 2013; Ulbrich et al. 2014; Liu et al. 2014; Hao et al. 2015).

For quantitative metabolomics, CIL LC–MS is performed using differential isotope labeling of individual samples (e.g., labeled with ^{12}C-reagent) and their control (e.g., labeled with ^{13}C-reagent), which overcomes the problems of matrix effect and ion suppression associated with MS detection (Guo and Li 2009, 2010). However, matrix compositions of individual samples such as the salt and buffer contents may be different from sample to sample or batch to batch. While it is important to control the sample collection and sample preparation steps properly for quantitative metabolomics, differences in sample matrix are unavoidable due to inherent variations of sample matrix such as salt contents in a biofluid (e.g., urine and

sweat) and logistical consideration in real world applications. An example of the latter is that samples may be collected at different centers or time under somewhat different conditions such as using different additives (buffers, EDTA, etc.). By necessity, one may want to profile these samples for improving the overall performance of a metabolomics study (e.g., using samples from different centers for biomarker validation after the initial work of disease biomarker discovery using a well-controlled sample set) (Dane et al. 2014). In another situation, valuable samples that have been subjected to NMR analysis may be re-used for MS-based profiling (Beltran et al. 2012). The NMR samples with the addition of phosphate buffer (PB) or phosphate buffer saline (PBS) that is used for controlling pH and ionic strength to minimize the chemical shift changes (Lauridsen et al. 2007; Asiago et al. 2008; Xiao et al. 2009; Akira et al. 2012) would obviously have different matrices from those of other untreated samples.

In this work, we report the presence of matrix effect on chemical labeling in a dansylation isotope labeling LC–MS metabolomic profiling workflow. We illustrate that metabolomic profiles of urine samples with and without the presence of high concentrations of NaCl, PB or PBS produced by dansylation LC–MS can be different. While matrix effect on LC–MS analysis can be overcome by differential CIL, this work points out the importance of using similar sample matrix for chemical labeling to maintain similar labeling efficiencies of individual metabolites in comparative metabolomics. We also demonstrate that for samples with varying concentrations of salts such as urine samples, simply diluting the samples to reduce the salt concentration prior to chemical labeling can overcome the matrix effect.

2 Materials and methods

2.1 Urine sample collection

Urine samples were collected from five age-matched healthy mice. Equal volumes of the five individual samples were mixed together to make a pooled sample. After sample collection, the urine samples were immediately stored in −80 °C freezer for further use.

2.2 Dansylation labeling

Supplemental Note N1 provides information on the chemical and reagents used. The frozen urine samples were thawed in an ice-bath and then centrifuged at 14,000 rpm for 15 min. 12.5 μL supernatant was taken into an Eppendorf tube and totally dried using a Speed Vac. The sample was re-dissolved to 50 μL with water or a specific matrix solution. Then 25 μL of 250 mM sodium carbonate/sodium bicarbonate buffer and 25 μL of ACN were added into the sample. The solution was vortexed, spun down, and mixed with 50 μL of freshly prepared ^{12}C-dansyl chloride solution in ACN (18 mg/mL) (for light labeling) or ^{13}C-dansyl chloride solution (18 mg/mL) (for heavy labeling). After 45 min incubation at 40 °C, 10 μL of 250 mM NaOH was added to the reaction mixture to quench the excess dansyl chloride. The solution was then incubated at 40 °C for another 10 min. Finally, formic acid (425 mM) in 50/50 ACN/H_2O was added to consume excess NaOH and to make the solution acidic. The ^{12}C- or ^{13}C-labeled sample was centrifuged at 14,000 rpm for 10 min before injecting onto LC–UV for quantification (Wu and Li 2012) (see Supplemental Note N1). For LC–MS analysis, the ^{12}C- and ^{13}C-labeled samples were mixed in equal amounts based on the LC–UV quantification results.

2.3 LC–FTICR–MS

LC–MS was performed using an Agilent 1100 series binary system (Agilent, Palo Alto, CA) with an Agilent reversed phase Eclipse Plus C18 column (2.1 mm × 100 mm, 1.8 μm particle size, 95 A pore size) that is connected to a Bruker 9.4 Tesla Apex-Qe Fourier transform ion-cyclotron resonance (FTICR) mass spectrometer (Bruker, Billerica, MA, USA) with electrospray ionization. All the MS measurements were done using positive ion mode. Supplemental Note N1 provides more information about the LC–MS conditions used. To monitor the instrumental performance, a quality control sample (i.e., a differentially labeled urine sample) was injected every 10–12 sample injections.

2.4 Data analysis

The LC–MS data are available from MetaboLights (www.ebi.ac.uk/metabolights/) (accession number MTBLS194). The ^{12}C/^{13}C peak pairs were extracted by the IsoMS software reported (Zhou et al. 2014). IsoMS-Align was used to align the peak pair data from different samples by retention time and accurate mass (Zhou et al. 2014). The missing values were filled back by using the Zero-fill program (Huan and Li 2015). Multivariate statistical analysis was carried out using SIMCA-P+ 12 (Umetrics AB, Umea, Sweden).

3 Results and discussion

3.1 Matrix effect on CIL

Differential CIL LC–MS provides relative quantification of metabolites in a sample versus a control of similar type

(e.g., an individual urine vs. a pooled urine) or absolute quantification of metabolites in a sample versus a list of standards with known concentrations. When the sample matrices are not identical, matrix effect during the labeling process may occur, which could decrease the quantification accuracy. To examine the matrix effect on dansylation labeling which targets the amine/phenol submetabolome, we analyzed five individual mouse urine samples and a pooled sample in triplicates. For each sample, 12.5 μL of sample were dried and then re-dissolved in 50 μL of PBS or water. The individual samples were separately labeled by ^{12}C-dansylation and the pooled sample was labeled by ^{13}C-dansylation. Note that the concentration of dansyl chloride which was in excess was kept the same for labeling samples; we did not investigate how different concentrations of dansyl chloride affect the labeling efficiency of a sample containing different concentrations of salts or buffers. In CIL LC–MS, as long as the labeling efficiency is consistent for labeling the samples and the pool, relative quantification can be performed without much error. The total metabolite concentrations of the labeled samples were measured by LC–UV for sample amount normalization before mixing.

Figure 1 shows the LC–UV measurement results where the peak area was determined from a chromatographic peak of all the dansyl labeled metabolites eluted by using high organic solvent in a step-gradient LC chromatogram. The concentration of the five urine samples could differ by as much as fivefold (sample #2 vs. sample #5). However, the total concentration of labeled metabolites is not affected by the presence or absence of PBS. Based on the LC–UV results alone, we could not detect any significant matrix effect on labeling. To normalize the sample amount for LC–MS analysis, equal amounts of a labeled sample and a labeled pooled sample were mixed. The same amount of the mixtures was injected into LC–MS for all samples. The intensity ratio of the ^{12}C-/^{13}C-labeled peaks from a metabolite peak pair in mass spectra was measured and entered into a metabolite-intensity table for the samples and all the metabolite peak pairs. Since the same pooled sample was used as a reference for all the individual samples, the peak ratios found in the table for a given metabolite reflect the relative concentration differences of the metabolite in these samples. This is the basis of quantitative metabolomics using differential CIL LC–MS.

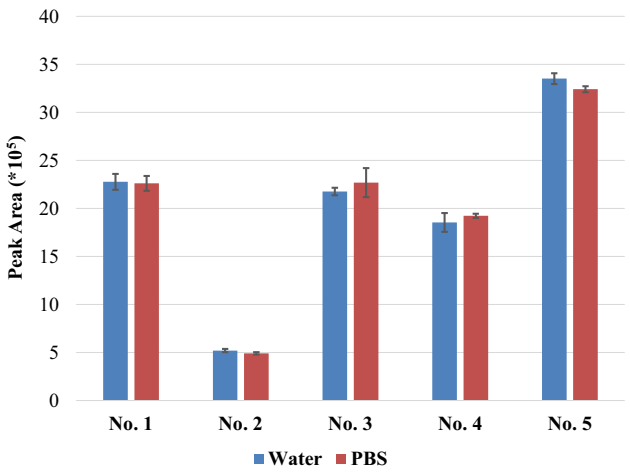

Fig. 1 LC–UV quantification of the total concentration of labeled metabolites in five mouse urine samples re-dissolved in water and PBS

For the triplicate analyses of five urine samples, a total of 1662 peak pairs or putative metabolites were detected. We applied partial least squares discriminant analysis (PLS-DA) and orthogonal projections to latent structures discriminant analysis (OPLS-DA) to these data to study the metabolomic changes. Figure 2 shows the score plots. As Fig. 2 shows, there is a significant difference among the mixtures of urine re-dissolved in PBS labeled by ^{12}C-dansylation and the pooled urine re-dissolved in H_2O labeled by ^{13}C-dansylation (denoted as the PBS/H_2O group), ^{12}C-urine in H_2O and ^{13}C-pooled-urine in PBS (i.e., H_2O/PBS group), and ^{12}C-urine in H_2O and ^{13}C-pooled-urine in H_2O (i.e., H_2O/H_2O group). The PBS/H_2O group and the H_2O/PBS group are clearly separated from the H_2O/H_2O group.

At the individual metabolite ratio level, taking urine #1 as an example, out of 1622 peak pairs detected, 402 pairs in PBS have peak ratios decreased by more than 15 %, compared to those in H_2O, while 396 pairs have ratios increased by more than 15 % (see Supplemental Figure S1 for the peak pair number distribution as a function of the peak ratios). Figure 3 shows four representative metabolites as an example to illustrate the matrix effect on labeling efficiency. Supplemental Table T1 shows the *p* values from *T* test of the peak ratios found in a given matrix group versus the H_2O/H_2O group. The labeling efficiency of creatine was slightly increased in PBS, resulting in higher PBS/H_2O ratio and lower H_2O/PBS ratio. In contrast, labeling of leucine, lysine and tyrosine was suppressed by the PBS matrix. Because labeling efficiency of individual metabolites may increase or decrease, the total concentration of labeled metabolites was not affected by the presence of PBS as shown in Fig. 1.

The results of PLS-DA and OPLS-DA plots and individual peak ratios clearly demonstrate that there was a matrix effect during the dansylation labeling process caused by the presence of PBS in a sample. Figure 2 also shows that the H_2O/H_2O group and the PBS/PBS group are overlapped on the score plots. The peak ratios of the four metabolites shown in Fig. 3 are similar for the two groups. These results indicate that, while there was a matrix effect,

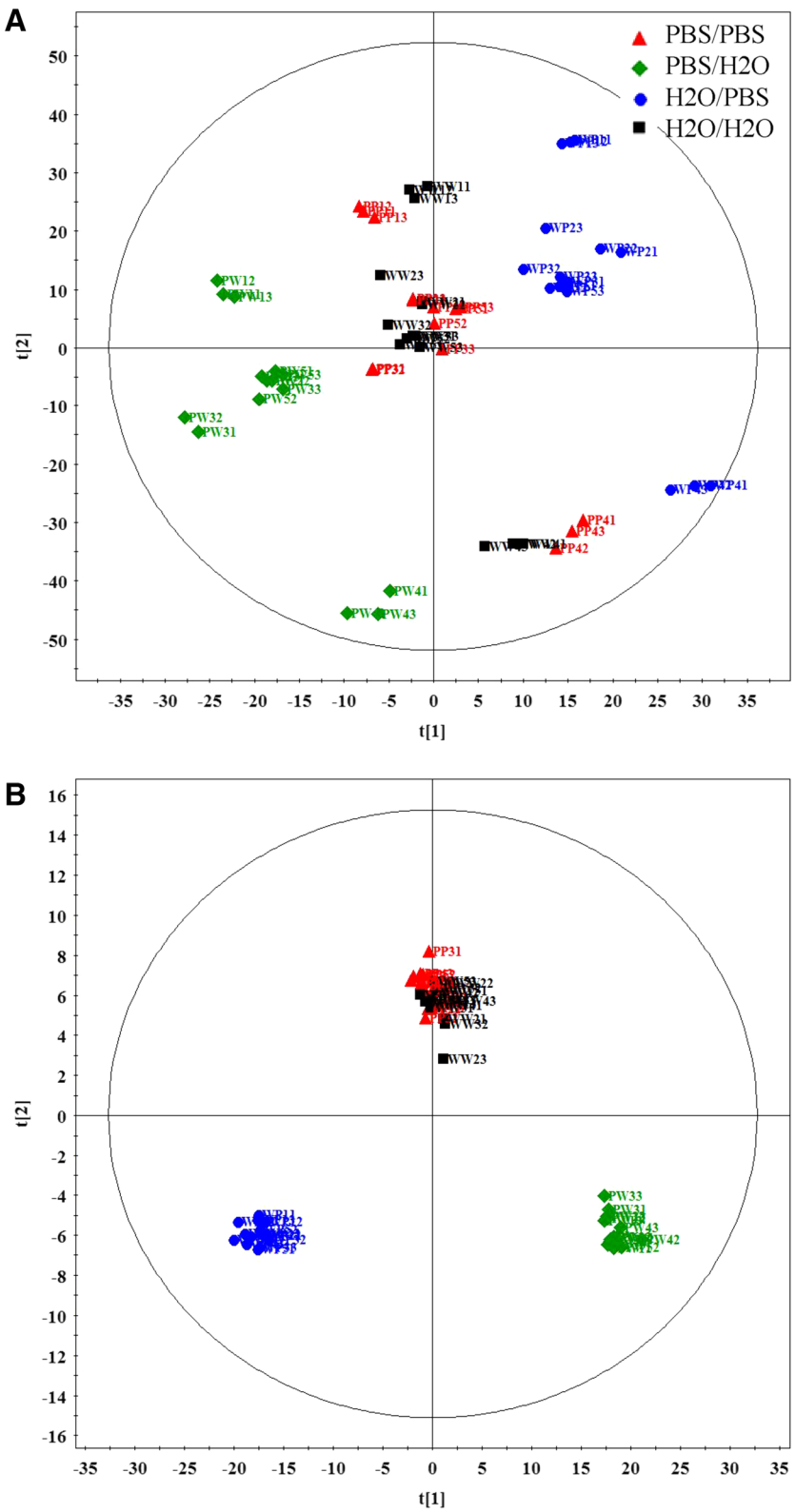

Fig. 2 **a** PLS-DA and **b** OPLS-DA score plots of dansylation LC-MS data obtained from five ^{12}C-dansylated mouse urine samples mixed with a ^{13}C-dansylated pooled sample. For each sample, three experimental replicates were performed. Label X/Y (X, Y = water or PBS) denotes a mixture of an individual urine re-dissolved in X and labeled with ^{12}C-dansylation and a pooled urine re-dissolved in Y and labeled with ^{13}C-dansylation

the relative quantification results of metabolites was not affected if the individual samples and the pooled sample had the same or similar matrix.

To confirm the presence of matrix effect and investigate how it can influence absolute metabolite quantification, we chose tyrosine, which had a 39 % peak ratio decrease in

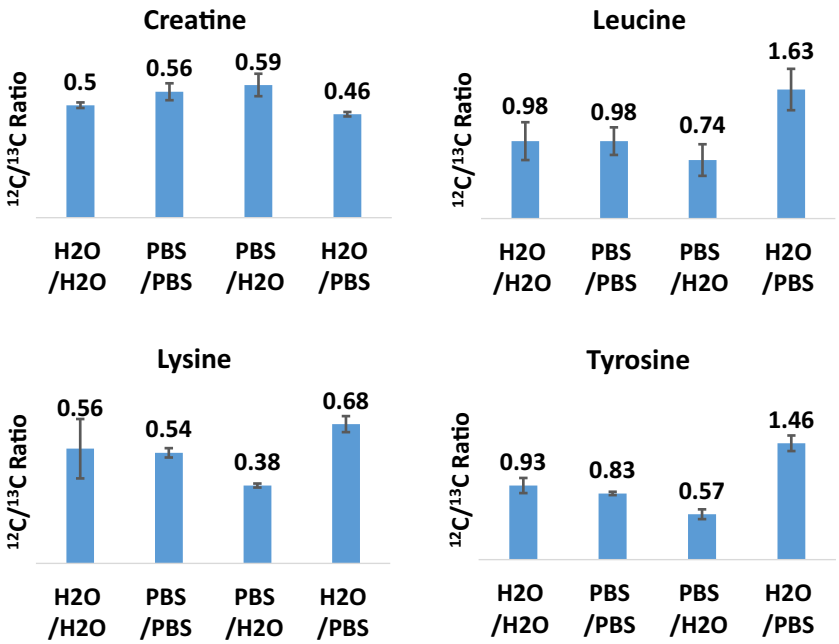

Fig. 3 Relative intensities of four representative metabolites in urine #1 versus a pooled urine determined from experimental triplicate analysis of four different mixtures as shown in Fig. 2

PBS, to generate standard addition curves. In this case, 12.5 µL of urine #1 was dried and re-dissolved to 50 µL using either PBS or water spiked with 1, 2, 3 and 4 µM tyrosine standard solutions. The samples were separately labeled, followed by LC–MS analysis. The area of dansyl-tyrosine peak (m/z 324.5953) was measured and plotted as a function of the concentration of spiked tyrosine. Figure 4a shows two standard addition curves for urine in PBS and water, respectively. There was a matrix effect on the labeling of tyrosine, causing a 35 % decrease in labeling efficiency. However, the same absolute concentration (2.16–2.17 µM) was found from the two curves. It is clear that there was a matrix effect on metabolite quantification which could be overcome by the standard addition method.

3.2 Origin of the matrix effect

To find a way to minimize the matrix effect on CIL, it is important to understand the origin and possible mechanism of this phenomenon. PBS solution contains 10 mM PB, 137 mM NaCl and 2.7 mM KCl. At first, we wanted to study PB and NaCl individually to see which one of them mostly contributes to the matrix effect in PBS. Because of the interest of performing MS analysis of the same sample already subjected to NMR measurement in our future research, we also examined the effect of a higher concentration PB, i.e., 50 mM. It should be noted that, using the tube-in-tube method (Tukiainen et al. 2008; Salek et al.

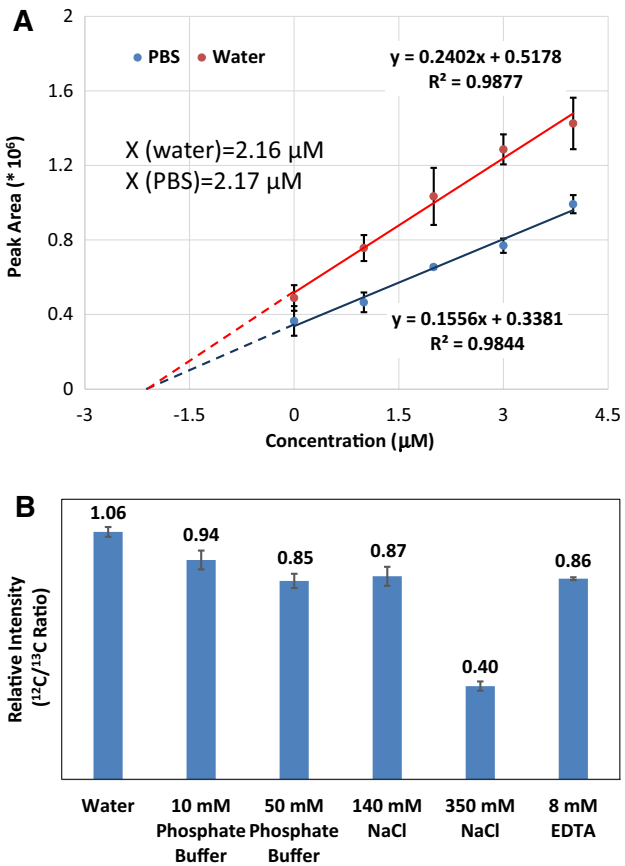

Fig. 4 **a** Standard addition curves for tyrosine in mouse urine labeled in water and PBS. **b** Comparison of relative intensities of tyrosine labeled in different matrices

2011; Glaves et al. 2014), no isotopic solvent needs to be added to the NMR sample and thus the sample, albeit containing high salt or buffer, can be readily transferred for MS analysis without any interference caused by the isotope solvent. Finally, 8 mM EDTA, which is approximately the final concentration of anticoagulant used in plasma, was also added to the list to examine its effect on labeling efficiency.

In our experiments, we dissolved tyrosine separately in water, 10 and 50 mM PB, 140 and 350 mM NaCl, and 8 mM EDTA, followed by labeling with ^{12}C-dansyl chloride and then 1:1 mixing with tyrosine in water labeled by ^{13}C-dansyl chloride. Note that dansyl chloride is highly soluble in acetonitrile or in a mixture of water and acetonitrile. As we increased the salt or buffer concentration in the dansyl chloride solution, we did not observe any precipitation. Thus the presence of varying concentrations of salts or buffers in the sample did not change the solubility of dansyl chloride. The peak pair ratios of tyrosine were calculated after LC–MS analysis and the results are shown in Fig. 4b. Supplemental Table T2 shows the *p* values from *T* test of the peak ratios found in a given matrix versus H_2O. As Fig. 4b shows, 140 mM NaCl has a larger effect on labeling efficiency, compared to 10 mM PB. The matrix effect of 50 mM PB is similar to that of 140 mM NaCl. More significantly, the tyrosine labeling efficiency in 350 mM NaCl solution is greatly reduced. In addition, 8 mM EDTA also causes matrix effect on tyrosine labeling to an extent similar to 50 mM PB or 140 mM NaCl.

Although keeping the alkaline environment is crucial for the dansylation reaction (Guo and Li 2009), no significant pH change of the reaction mixture was observed for these samples. Hence, the buffering property of PBS or PB was not the reason causing the matrix effect. Considering the results of the two NaCl samples (140 vs. 350 mM), we argue that increasing ionic strength in the labeling solution by high concentration of salts might be the main cause of the matrix effect. In the case of phosphate buffer, since HPO_4^{2-} carries two charges, the ionic strength of PB should be higher than NaCl solution at the same concentration. However, the concentration of Na_2HPO_4/KH_2PO_4 in PBS is much lower than NaCl. Therefore, the matrix effect of PBS could be considered mainly as the matrix effect of the salt. The 8 mM EDTA solution contains only 16 mM Na^+, but the matrix effect was also observed. This could be the effect of EDTA anion, which carries more charges than sodium cation.

To further examine how salt content or ionic strength can affect the labeling reaction, we dissolved a mixture of equal amounts of 16 amino acid standards in NaCl solution at a concentration ranging from 0 to 650 mM. When the salt concentration increased to 750 mM, acetonitrile and water could be separated into two layers by centrifuging. This is because the salt ions weaken the interaction between water molecules and acetonitrile molecules and change the solvent into an emulsion. This layer separation should be avoided for carrying out the labeling reaction. The amino acid mixture dissolved in different concentrations of NaCl was separately labeled by ^{12}C-dansyl chloride and then 1:1 mixed with a control standard labeled with ^{13}C-dansyl chloride in water. The peak pair ratios were calculated and plotted against the concentration of NaCl and the results are shown in Fig. 5. As Fig. 5 shows, the 16 amino acids have different responses to the increasing salt concentration. The eight relatively hydrophilic dansyl-amino acids (Fig. 5a, b) have less effect by increasing NaCl concentration. However, the peak pair ratios of the relatively hydrophobic dansyl-amino acids except dansyl-cystine decrease significantly as the salt concentration increases (Fig. 5c, d). For example, the peak pair ratio of dansyl-tyrosine in 650 mM NaCl is only about 24 % of the ratio determined in water.

The fact that relatively hydrophobic amino acids are more sensitive to the salt matrix supports our hypothesis on the role of ionic strength on matrix effect. Carta and Tola reported the solubility of glycine, leucine, cystine and tyrosine in aqueous solution at different NaCl concentrations (Carta and Tola 1996). As the NaCl concentration increases, the solubility of cystine increases, while the solubility of leucine and tyrosine decreases. Glycine solubility is not affected by the salt. Our results of matrix effect on the hydrophobic amino acids follow a similar trend. Dansylation reaction between dansyl chloride and an amine-containing metabolite is initiated by nucleophilic attack of the amine to the dansyl sulfide. An intermediate or ion pair of dansyl and chloride is formed, followed by substitution of chloride by the amine (see Supplemental Figure S2). Ionic strength can influence the nucleophilic attack. Any ionic species from a matrix that surround the dansyl moiety may reduce or enhance the propensity of the amine to interact with dansyl to form a product, resulted in an decrease or increase in labeling efficiency. For amino acids with hydrophobic side chains, increasing ionic strength makes them more difficult to interact with the dansyl moiety, which reduces the dansylation efficiency.

3.3 Minimizing the matrix effect on metabolomic profiling

From the above results and discussion, it is apparent that high salts in various forms such as NaCl, PB or PBS can cause matrix effect on dansylation labeling. PB or PBS is introduced during sample preparation for various reasons. On the other hand, salts such as NaCl are inherently present at high concentrations in several biofluids such as urine and sweat. The salt concentration can vary from sample to

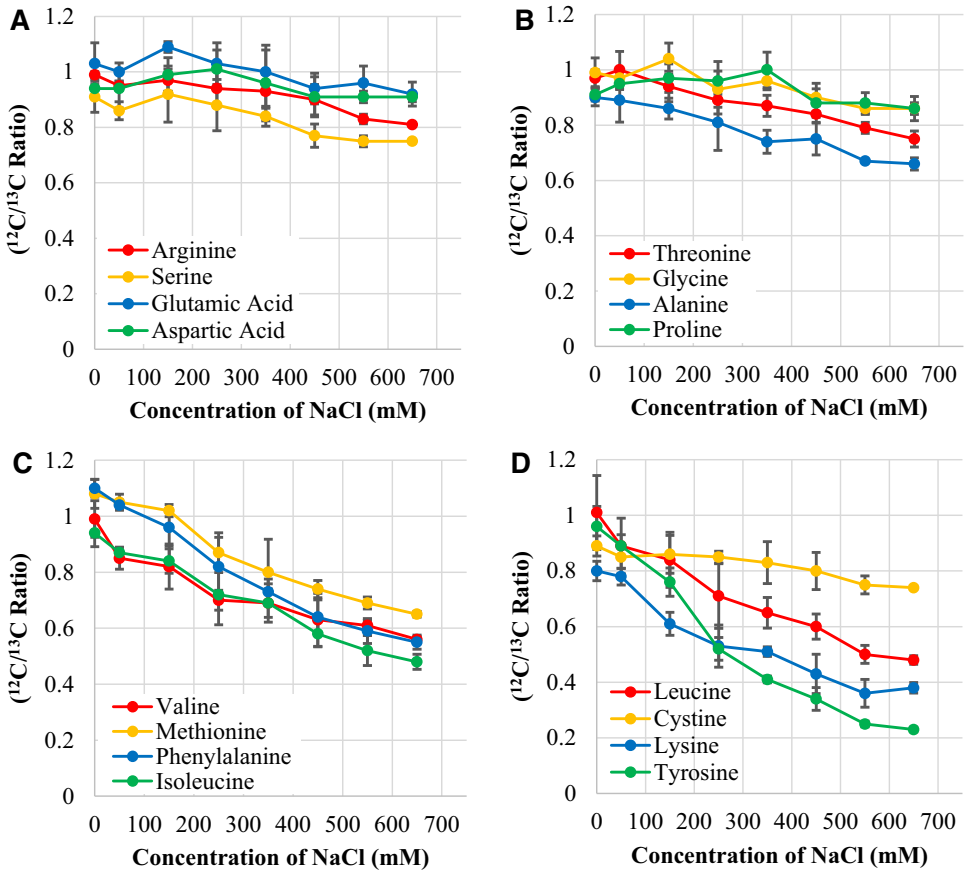

Fig. 5 Relative intensities of 16 amino acids as a function of NaCl concentration in the sample solution

sample. For example, in the study of urine sodium excretion trend between 1988 and 2010 among U.S. adults (age 20–59 years) (Pfeiffer et al. 2014), the urine sodium concentrations in spot urine specimens were reported to be 111 mM (mean) with 22.8 mM at 5th percentiles, 103 mM at 50th percentiles, and 221 mM at 95th percentiles for 1249 adults collected between 1988 and 1994. Slight increases in urine sodium concentrations were found for 1235 adults collected between 2003 and 2006 and 525 adults in 2010. The potassium concentrations in human urine are less than 1/3 of the sodium levels (Donfrancesco et al. 2013) and other metal ions concentrations are even lower (Sieniawska et al. 2012). For mouse urine samples, the sodium concentration can range from ~40 to ~150 mM and the potassium concentrations can range from ~150 to ~500 mM, depending on the diet and age (Schmidt et al. 2013).

To examine how the salt contents can affect the metabolomic profiling, we selected one mouse urine and then diluted by fivefold using different concentrations of NaCl solutions (50, 150, 250 and 350). All these urine samples were labeled by ^{12}C-dansyl chloride and then mixed with a control sample diluted by water which was ^{13}C-dansylated. After LC–MS analysis, 1294 peak pairs or putative metabolites were detected. Figure 6a shows the PLS-DA score plot of the samples. There is a positive correlation between the salt concentration and the matrix effect. The higher the salt concentration, the further the data points separated from the sample diluted by water. After adding the results from the un-diluted sample to the plot, Fig. 6b shows the new plot. The samples diluted by water, 50 mM NaCl, 150 mM NaCl cluster together. The samples diluted by 250 and 350 mM are clearly separated from the other diluted samples. The undiluted urine is significantly different from the fivefold water diluted sample. These results indicate that the high salt concentration in the original urine had a strong matrix effect. After fivefold dilution using water or low salt solution (50 mM), the matrix effect is greatly reduced or eliminated. Therefore, a dilute-then-label approach can be used to overcome the matrix effect on the CIL of biofluid samples. Figure 6a, b indicates that the presence of 50 mM NaCl in the urine samples does not cause significant matrix effect. This result is consistent with the data shown in Fig. 5 where the peak ratios of most of the labeled metabolites do not differ significantly between the water and 50 mM NaCl samples.

The effects of varying concentrations of PBS were also examined. Similar trend to those of NaCl samples was observed for these samples (see Fig. 6c). The samples labeled in fourfold diluted PBS (2.5 mM phosphate buffer

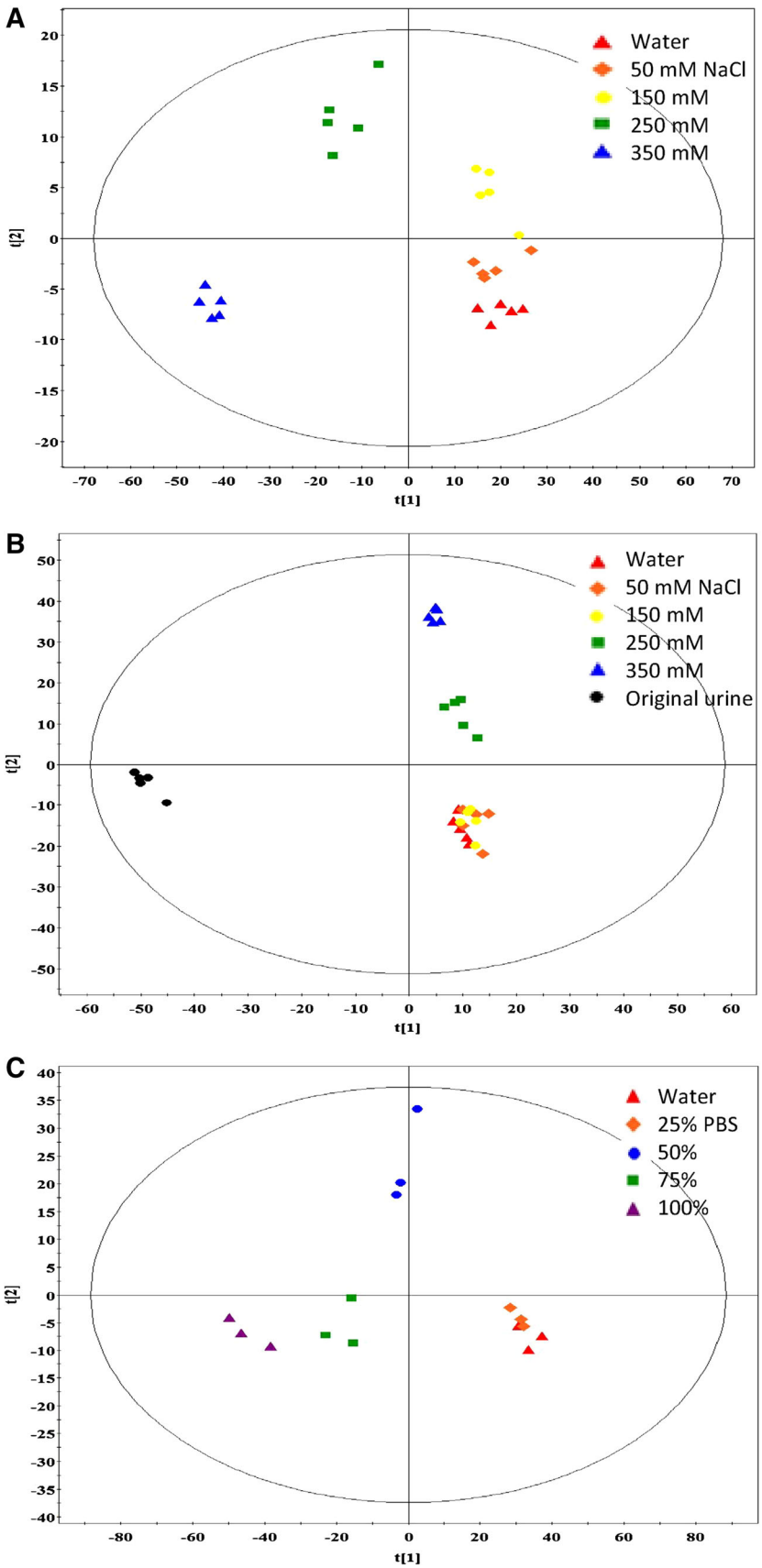

Fig. 6 **a** PLS-DA score plot for fivefold diluted urine #1 labeled in water (*red*) and NaCl solutions (50 mM in *orange*, 150 mM in *yellow*, 250 mM in *green*, and 350 mM in *blue*). **b** PLS-DA score plot for the comparison of an undiluted urine sample labeled with dansylation (*black*) and fivefold diluted urine samples labeled in water and NaCl solutions. The injection amount for all the samples based on LC–UV measurement was the same. **c** PLS-DA score plot for the comparison of fourfold diluted urine #1 labeled at different concentrations of PBS solution (e.g., 25 % PBS refers to fourfold dilution of the PBS solution). For each sample, five experimental replicates were performed in **a** and **b**, while three experimental replicates were performed in **c**

and 35 mM NaCl) are inseparable from the water-diluted samples as shown in Fig. 6c. As the PBS concentration increases, the matrix effect becomes more significant. These results suggest that, for an NMR sample containing high concentration of PBS, we can simply dilute it to minimize the matrix effect on CIL LC–MS.

4 Concluding remarks

We demonstrated the presence of matrix effect on chemical labeling that could affect the quantitative metabolomic profiling results in CIL LC–MS. Relative metabolite quantification in differential CIL LC–MS was not affected, if the same or similar matrix was present in comparative metabolomic samples. Because matrix effect is only present when the salt or buffer concentration is very high such as in some urine samples, the simplest way to minimize the influence of matrix effect on quantitative metabolomic profiling is to dilute all the samples by a specific fold (e.g., fourfold or fivefold for urine samples). Over-dilution is not recommended as it can increase the time required for concentrating the labeled samples in downstream processing. For different types of biofluids as well as different labeling chemistries, matrix effect on the chemical labeling process might be different and thus examining the matrix effect should be part of the protocol development for CIL LC–MS based metabolomics.

Acknowledgments This work was funded by the Natural Sciences and Engineering Research Council of Canada, the Canadian Institutes for Health Research, the Canada Research Chairs program, Genome Canada, Genome Alberta and Alberta Innovates.

Compliance with Ethical Standards

Ethical Approval All institutional and national guidelines for the care and use of laboratory animals were followed.

Conflict of interest The authors declared that they have no conflict of interest in the submission of this manuscript.

References

Akira, K., Hichiya, H., Shuden, M., Morita, M., & Mitome, H. (2012). Sample preparation method to minimize chemical shift variability for NMR-based urinary metabonomics of genetically hypertensive rats. *Journal of Pharmaceutical and Biomedical Analysis, 66*, 339–344.

Asiago, V. M., Gowda, G. A. N., Zhang, S., Shanaiah, N., Clark, J., & Raftery, D. (2008). Use of EDTA to minimize ionic strength dependent frequency shifts in the (1)H NMR spectra of urine. *Metabolomics, 4*(4), 328–336.

Beltran, A., Suarez, M., Rodriguez, M. A., Vinaixa, M., Samino, S., Arola, L., et al. (2012). Assessment of compatibility between extraction methods for NMR- and LC/MS-based metabolomics. *Analytical Chemistry, 84*(14), 5838–5844.

Bruheim, P., Kvitvang, H. F. N., & Villas-Boas, S. G. (2013). Stable isotope coded derivatizing reagents as internal standards in metabolite profiling. *Journal of Chromatography A, 1296*, 196–203.

Bueschl, C., Krska, R., Kluger, B., & Schuhmacher, R. (2013). Isotopic labeling-assisted metabolomics using LC-MS. *Analytical and Bioanalytical Chemistry, 405*(1), 27–33.

Carta, R., & Tola, G. (1996). Solubilities of L-cystine, L-tyrosine, L-leucine, and glycine in aqueous solutions at various pHs and NaCl concentrations. *Journal of Chemical and Engineering Data, 41*(3), 414–417.

Dai, W. D., Huang, Q., Yin, P. Y., Li, J., Zhou, J., Kong, H. W., et al. (2012). Comprehensive and highly sensitive urinary steroid hormone profiling method based on stable isotope-labeling liquid chromatography mass spectrometry. *Analytical Chemistry, 84*(23), 10245–10251.

Dane, A. D., Hendriks, M., Reijmers, T. H., Harms, A. C., Troost, J., Vreeken, R. J., et al. (2014). Integrating metabolomics profiling measurements across multiple biobanks. *Analytical Chemistry, 86*(9), 4110–4114.

Donfrancesco, C., Ippolito, R., Lo Noce, C., Palmieri, L., Iacone, R., Russo, O., et al. (2013). Excess dietary sodium and inadequate potassium intake in Italy: Results of the MINISAL study. *Nutrition Metabolism and Cardiovascular Diseases, 23*(9), 850–856.

Fu, F. F., Cheng, V. W. T., Wu, Y. M., Tang, Y. A., Weiner, J. H., & Li, L. (2013). Comparative proteomic and metabolomic analysis of Staphylococcus warneri SG1 cultured in the presence and absence of butanol. *Journal of Proteome Research, 12*(10), 4478–4489.

Glaves, J. P., Li, M. X., Mercier, P., Fahlman, R. P., & Sykes, B. D. (2014). High-throughput, multi-platform metabolomics on very small volumes: H-1 NMR metabolite identification in an unadulterated tube-in-tube system. *Metabolomics, 10*(6), 1145–1151.

Guo, K., & Li, L. (2009). Differential C-12/C-13-isotope dansylation labeling and fast liquid chromatography/mass spectrometry for absolute and relative quantification of the metabolome. *Analytical Chemistry, 81*(10), 3919–3932.

Guo, K., & Li, L. (2010). High-performance isotope labeling for profiling carboxylic acid-containing metabolites in biofluids by mass spectrometry. *Analytical Chemistry, 82*(21), 8789–8793.

Hao, L., Zhong, X. F., Greer, T., Ye, H., & Li, L. J. (2015). Relative quantification of amine-containing metabolites using isobaric N,N-dimethyl leucine (DiLeu) reagents via LC-ESI-MS/MS and CE-ESI-MS/MS. *Analyst, 140*(2), 467–475.

Huan, T., & Li, L. (2015). Counting missing values in a metabolite-intensity data set for measuring the analytical performance of a metabolomics platform. *Analytical Chemistry, 87*(2), 1306–1313.

Lauridsen, M., Hansen, S. H., Jaroszewski, J. W., & Cornett, C. (2007). Human urine as test material in H-1 NMR-based metabonomics: Recommendations for sample preparation and storage. *Analytical Chemistry, 79*(3), 1181–1186.

Leng, J. P., Wang, H. Y., Zhang, L., Zhang, J., Wang, H., & Guo, Y. L. (2013). A highly sensitive isotope-coded derivatization method and its application for the mass spectrometric analysis of analytes containing the carboxyl group. *Analytica Chimica Acta, 758*, 114–121.

Liu, P., Huang, Y. Q., Cai, W. J., Yuan, B. F., & Feng, Y. Q. (2014). Profiling of thiol-containing compounds by stable isotope labeling double precursor ion scan mass spectrometry. *Analytical Chemistry, 86*(19), 9765–9773.

Pfeiffer, C. M., Hughes, J. P., Cogswell, M. E., Burt, V. L., Lacher, D. A., LaVoie, D. J., et al. (2014). Urine sodium excretion increased slightly among US adults between 1988 and 2010. *Journal of Nutrition, 144*(5), 698–705.

Salek, R., Cheng, K. K., & Griffin, J. (2011). The study of mammalian metabolism through nmr-based metabolomics. In D. Jameson, M. Verma, & H. V. Westerhoff (Eds.), *Methods in enzymology. Methods in systems biology* (Vol. 500, pp. 337–351). San Diego: Elsevier Academic Press Inc.

Schmidt, K., Ripper, M., Tegtmeier, I., Humberg, E., Sterner, C., Reichold, M., et al. (2013). Dynamics of renal electrolyte excretion in growing mice. *Nephron Physiology, 124*(3–4), 7–13.

Sieniawska, C. E., Jung, L. C., Olufadi, R., & Walker, V. (2012). Twenty-four-hour urinary trace element excretion: Reference intervals and interpretive issues. *Annals of Clinical Biochemistry, 49*, 341–351.

Tang, Z. M., & Guengerich, F. P. (2010). Dansylation of unactivated alcohols for improved mass spectral sensitivity and application to analysis of cytochrome P450 oxidation products in tissue extracts. *Analytical Chemistry, 82*(18), 7706–7712.

Tayyari, F., Gowda, G. A. N., Gu, H. W., & Raftery, D. (2013). N-15-Cholamine-A smart isotope tag for combining NMR- and MS-based metabolite profiling. *Analytical Chemistry, 85*(18), 8715–8721.

Toyo'oka, T. (2012). LC-MS determination of bioactive molecules based upon stable isotope-coded derivatization method. *Journal of Pharmaceutical and Biomedical Analysis, 69*, 174–184.

Tukiainen, T., Tynkkynen, T., Makinen, V. P., Jylanki, P., Kangas, A., Hokkanen, J., et al. (2008). A multi-metabolite analysis of serum by H-1 NMR spectroscopy: Early systemic signs of Alzheimer's disease. *Biochemical and Biophysical Research Communications, 375*(3), 356–361.

Ulbrich, A., Bailey, D. J., Westphall, M. S., & Coon, J. J. (2014). Organic acid quantitation by NeuCode methylamidation. *Analytical Chemistry, 86*(9), 4402–4408.

Wu, Y. M., & Li, L. (2012). Determination of total concentration of chemically labeled metabolites as a means of metabolome sample normalization and sample loading optimization in mass spectrometry-based metabolomics. *Analytical Chemistry, 84*(24), 10723–10731.

Xiao, C. N., Hao, F. H., Qin, X. R., Wang, Y. L., & Tang, H. R. (2009). An optimized buffer system for NMR-based urinary metabonomics with effective pH control, chemical shift consistency and dilution minimization. *Analyst, 134*(5), 916–925.

Yuan, W., Zhang, J. X., Li, S. W., & Edwards, J. L. (2011). Amine metabolomics of hyperglycemic endothelial cells using capillary LC-MS with isobaric tagging. *Journal of Proteome Research, 10*(11), 5242–5250.

Zhou, R., Tseng, C. L., Huan, T., & Li, L. (2014). IsoMS: automated processing of LC-MS data generated by a chemical isotope labeling metabolomics platform. *Analytical Chemistry, 86*(10), 4675–4679.